



UNIVERSITÀ
DEGLI STUDI
FIRENZE

FLORE

Repository istituzionale dell'Università degli Studi di Firenze

Experimental study of the wind pressure field on the Notre Dame Cathedral in Paris

Questa è la Versione finale referata (Post print/Accepted manuscript) della seguente pubblicazione:

Original Citation:

Experimental study of the wind pressure field on the Notre Dame Cathedral in Paris / Claudio Mannini, Tommaso Massai, Enrico Panettieri, Niccolò Barni, Andrea Giachetti, Margherita Ferrucci, Marco Montemurro, Paolo Vannucci. - In: INTERNATIONAL JOURNAL OF ARCHITECTURAL HERITAGE. - ISSN 1558-3066. - STAMPA. - 18:(2024), pp. 194-214. [10.1080/15583058.2022.2136022]

Availability:

The webpage <https://hdl.handle.net/2158/1283459> of the repository was last updated on 2025-11-02T11:17:10Z

Published version:

DOI: 10.1080/15583058.2022.2136022

Terms of use:

Open Access

La pubblicazione è resa disponibile sotto le norme e i termini della licenza di deposito, secondo quanto stabilito dalla Policy per l'accesso aperto dell'Università degli Studi di Firenze (<https://www.sba.unifi.it/upload/policy-oa-2016-1.pdf>)

Publisher copyright claim:

La data sopra indicata si riferisce all'ultimo aggiornamento della scheda del Repository FloRe - The above-mentioned date refers to the last update of the record in the Institutional Repository FloRe

(Article begins on next page)

1 **Experimental study of the wind pressure field on the Notre**
2 **Dame Cathedral in Paris**

3 Claudio Mannini¹, Tommaso Massai¹, Enrico Panettieri², Niccolò Barni¹, Andrea Giachetti¹,
4 Margherita Ferrucci³, Marco Montemurro², and P. Vannucci*⁴

¹CRIACIV-Department of Civil and Environmental Engineering, University of Florence,
5 Via S. Marta, 3, 50139 Florence, Italy

6 ²Arts et Métiers Institut of Technology - Université de Bordeaux, CNRS, INRA, Bordeaux INP,
7 HESAM Université, I2M UMR5295, 33405 Talence, France.

8 ³ Laboratorio di Fisica Tecnica Ambientale, Università IUAV, 30135 Venezia, Italy.

9 ⁴LMV - UMR8100, Université Paris-Saclay - UVSQ. 45, Avenue des Etats-Unis,
78035 Versailles, France.

10 August 31, 2022

11 **Abstract**

12 The paper concerns an experimental study on the wind pressures over the surface
13 of a worldwide known Gothic Cathedral: Notre Dame of Paris. The experimental
14 tests have been conducted in the CRIACIV wind tunnel, Prato (Italy), on a model
15 of the Cathedral at the scale 1:200 reproducing the atmospheric boundary layer.
16 Two types of tests have been conducted: with or without the surrounding modeling
17 the part of the city of Paris near the Cathedral. This has been done, on the one
18 hand, for evaluating the effect of the surrounding buildings onto the wind pressure

*Corresponding author: paolo.vannucci@uvsq.fr

19 distribution on the Cathedral, and, on the other hand, to have a wind pressure
20 distribution plausible for any other Cathedral with a similar shape. The tests have
21 been done for all the wind directions and the mean and peak pressures have been
22 recorded. The results emphasize that the complex geometry of this type of structures
23 is responsible for a peculiar aerodynamic behavior that does not allow estimating
24 correctly the wind loads on the various parts of the Cathedral based on codes and
25 standards, which are tailored for ordinary regular buildings.

26 **Key words:** Gothic Cathedral, Notre Dame, wind pressure, wind tunnel tests,
27 climate change effects, additive manufacturing.

28 1 Introduction

29 The scientific research on built heritage is more and more pushed by environmental prob-
30 lems, such as the climate change (Orr et al. 2021), which represents an increasing threat
31 for its preservation. Some recent, still ongoing, research projects testify of the importance
32 of the relationship between built heritage and climate change and of the increasing inter-
33 est of governments, supranational organizations, conscious that the conservation of the
34 architectural heritage is linked to the fundamental values of the social and intellectual
35 life of the nations (Deland et al. 2020). We recall, for instance, the projects funded by
36 the European Union within the Joint Programming Initiative on Cultural Heritage and
37 Global Change and by the Cultural Heritage H2020-EU¹. In particular, the global warm-

¹HYPERION (Development of a Decision Support System for Improved Resilience and Sustainable Reconstruction of historic areas to cope with Climate Change and Extreme Events based on Novel Sensors and Modelling Tools);

ARCH (Advancing Resilience of Historic Areas against Climate-related and other Hazards);

CONSECH20 (CONSErvation of 20th century concrete Cultural Heritage in urban changing environments).

38 ing of Earth is causing more and more frequent and strong wind storms, which constitute
39 today (and will constitute) a severe threat for the conservation of some iconic monumental
40 structures. According to [Steenbergen et al. \(2012\)](#), the climate change implies an increase
41 up to 2.3% in the hourly mean wind speed with a return period of 50 years. An ade-
42 quate evaluation of the wind pressure on monumental structures is hence of paramount
43 importance for a correct safety evaluation of such structures in the next future.

44 This is even more stringent for high-rise buildings, like the Gothic Cathedrals, which
45 are more exposed to the action of wind, whose speed increases with the height above the
46 ground. An example of the increasing danger such monuments are exposed to, is the
47 damage to the great rose of the Cathedral of Soissons (France), destroyed by the storm
48 Egon on January 13th, 2017. Some minor damages were also suffered by other great
49 Gothic Cathedrals in France during the severe wind storms of the last days of December
50 1999, like the Notre Dame Cathedral in Paris, where a wind as strong as 169 km/h was
51 recorded inside the city. Famous is also the collapse of the Spire of Saint Bonifatius
52 Church in Leeuwarden, The Netherlands, during a wind storm in 1976. To this end,
53 this paper focuses on the evaluation of wind pressures on Gothic Cathedrals, which are a
54 major example of the built heritage in Europe.

55 Generally, four approaches are used to investigate the wind effects on structures in the
56 atmospheric boundary layer: theoretical studies, full-scale measurements, Computation
57 Fluid Dynamics (CFD) numerical simulations and physical experiments on reduced-scale
58 models. Theoretical models concern objects of simple, aerodynamic shape, and they
59 are not suited for complex structures like Gothic Cathedrals. Full-scale measurements
60 are very expensive and require the possibility of equipping with sensors the considered
61 structure. For these reasons, in wind engineering experimental campaigns *in situ* are

62 still scarce and often they serve to corroborate either the results of experiments on scale
63 models or the results of a computation. CFD numerical simulations are more and more
64 used in the study of the wind pressure and velocity fields around buildings. Although
65 they can provide detailed information on the relevant flow variables, their accuracy and
66 reliability are still of concern, especially when the simulations regard buildings with a
67 complicated shape, located in an urban environment, as in the case of Gothic Cathedrals.
68 In such situations, the validation of the studies by full-scale measurements or reduced-
69 scale experimental tests is necessary (Blocken 2014). Therefore, experiments on scale
70 physical models in wind tunnels, used since the early twentieth century (Ferrucci and
71 Peter 2020) remain still today an indispensable and reliable tool for a correct analysis of
72 the wind field around buildings of complicated geometry in an urban landscape.

73 Due to their dimensions and geometry, the fine detail and richness of their decorations,
74 their particular structural organization, composed by high vaults, flying buttresses, timber
75 roofing, and also due to the materials they are composed of (i.e., stone, mortar, stain-
76 glasses, wood), Gothic Cathedrals are very peculiar and quite delicate structures. The
77 use of some technical norms, e.g. Eurocode 1 (CEN 2004), in evaluating the wind load on
78 them, seems inadequate. Indeed, such norms are conceived for the design of ordinary new
79 buildings, while Gothic Cathedrals are existing and really extra-ordinary constructions. In
80 particular, the wind load prescribed by Eurocode 1 is very simplified and, for a complicated
81 structure, it is not possible to know whether it over- or under-estimates the real loading.
82 Therefore, it would be pretentious and rather unrealistic to assess the structural safety
83 of a Gothic Cathedral, in respect of the increasingly severe wind storms that are caused
84 by climate change, using so a rough model. Indeed, a deep scientific investigation of the
85 wind-induced pressure distribution on the surface of a Gothic Cathedral is necessary for

86 a correct risk assessment of such structures or of some parts of them. This is a scientific
87 challenge that still waits for an adequate response.

88 In the literature, experimental studies of the wind pressure field on a Cathedral, even
89 if not Gothic, are rare. A few works focus on the spires of Cathedrals, or on slender
90 structures similar to spires, or on masonry structures of particular value or architectural
91 interest; some of them are briefly recalled hereafter. To the authors' best knowledge, there
92 is only an old wind tunnel investigation on a bi-dimensional model of a Cathedral-like
93 building (Chien et al. 1951). Originally, this study did not concern Cathedrals or churches
94 in particular, but just buildings with some typical cross-section shapes, one of them being
95 similar to a simple model of the nave of a Middle Age church. Results were given in the
96 form of bi-dimensional diagrams of the wind pressure coefficient, as shown in Fig. 1, and
97 it has been the basis for some subsequent pioneer works on the matter made by R. Marks
98 and co-workers, e.g. Mark and Jonash (1970). Two studies on the dynamic response of
99 two slender masonry structures to wind actions, the San Gaudenzio Basilica in Novara and
100 the Mole Antonelliana in Turin (both in Italy), are cited in Calderini and Pagnini (2015).
101 For the latter, a storm caused the collapse of the spire in 1953, and its reconstruction
102 was undertaken only after wind tunnel tests in the Aeronautics Laboratory of the Turin
103 Polytechnic University in 1954. The wind pressure on the Church of Sainte-Jeanne-d'Arc
104 in Rouen (France) was determined by wind tunnel experiments in the Eiffel Laboratory
105 in Paris (Romani 1972). In Szalay (1983), a wind tunnel study for a damaged ancient
106 church spire is proposed, in order to evaluate the wind load to be used for the design of
107 the reinforcing structure. The experiments were performed in the Hungarian Institute of
108 Building Science. The investigation about the wind effects on the leaning Tower of Pisa
109 (Italy) is described in Solari et al. (1998). The experiments were devoted to understand

110 the wind load that could cause the collapse of the tower due to the weak strength of the
111 foundation soil. The wind-induced pressures on the monumental roof structure of the XII
112 century Palazzo della Ragione in Padova were also experimentally studied in [Borri and](#)
113 [Facchini \(1999\)](#). The tests were performed in the CRIACIV wind tunnel Laboratory in
114 Prato (Italy). More recently, in a study on the vulnerability of the Capetian architecture
115 to wind storms ([Brocato et al. 2016](#)), CFD simulations were carried out on 2D simplified
116 models of some churches. In [Domede et al. \(2019\)](#), the wind load provided by Eurocode 1
117 is compared to the ancient methods available at the time of the construction (end of XIX
118 century) of the Ile Vierge Lighthouse (France), the tallest stone lighthouse in Europe.

119 As far as Gothic Cathedrals are specifically concerned, there are very few studies on
120 the wind actions: this is rather surprising, being these structures sensitive to wind storms
121 due to their height and large dimensions. Usually, the structure of the Cathedral is
122 modeled through a simple bi-dimensional scheme and analyzed with different techniques:
123 the line of pressure method in [Ungewitter \(1890\)](#); photo-elasticity in [Mark and Jonash](#)
124 [\(1970\)](#), [Mark \(1982; 1984\)](#); limit analysis in [Como \(2013\)](#) and [Coccia et al. \(2015\)](#). The
125 only work on the wind strength of a Gothic Cathedral considering a three-dimensional,
126 though partial, model and a nonlinear material behavior is a recent paper ([Vannucci et al.](#)
127 [2019](#)). Just as an example, Fig. 1 shows the wind load on a Cathedral-like construction
128 as suggested in [Chien et al. \(1951\)](#) and how this is applied to a bi-dimensional Cathedral
129 model in [Mark and Jonash \(1970\)](#). In all of the works cited above, the wind pressure is
130 simply modeled as a uniform or linearly variable load. Also in a recent study about the
131 roofing structure of Notre Dame in Paris, destroyed by the fire of April 15th, 2019, the
132 wind load is assumed as step-wise uniform ([Vannucci 2021](#)).

133 The present work is an experimental study that aims at providing an extensive evalu-

134 ation of the wind load that can be expected on the various parts of a Gothic Cathedral.
135 Such a study is clearly still missing in the literature, and without any doubt it is a fun-
136 damental step for a correct evaluation of the structural safety of such monuments. The
137 experimental investigation is carried out in a boundary-layer wind tunnel on a physical
138 scale model of the Cathedral of Notre Dame in Paris, an emblematic building of the French
139 Gothic age.

140 The goal of the present study is twofold. Firstly, it aims at providing a precise portrait
141 of the wind pressure field on this iconic construction, which has been the objective of many
142 discussions and structural analyses after the infamous recent fire that destroyed the roof,
143 the spire and damaged parts of the vaults. Secondly, regarding the assessment of the
144 wind effects, Notre Dame in Paris can be seen as a sort of paradigm of a more generic
145 Gothic Cathedral. Thus, an emphasis is put on the influence of the specific surrounding
146 built environment on the pressure field and, by consequence, the tests are made with or
147 without the surrounding city environment.

148 It is worth noting that this experimental study is performed not only on an extremely
149 precise physical model of the Cathedral, realized through 3D-printing, but also, and this
150 constitutes a scientific primacy, on a highly instrumented model. Thanks to a careful and
151 very dense distribution of pressure captors, a fine reconstruction of the wind load on the
152 various parts of a Gothic Cathedral has thus been possible for the first time.

2 Fabrication technology and materials of the Cathedral's model

The campaign of experimental tests has been done on a physical model of the Cathedral at the scale of 1:200. This scale has been chosen accounting for the dimensions of the Cathedral (130 m long, 45 m wide, 44 m high at the roof's top and 96 m at the spire's top) in order to satisfy a number of requirements. On the one hand, the model should be as large as possible to allow for a finer reproduction of the complex geometry of the structure and to facilitate the installation of a large number of pressure taps in all of its parts (see Section 2.2). On the other hand, the model must be "small" compared to the wind tunnel test chamber (2.4 m wide and 1.6 m high in the present case) not to alter the flow field around the construction (blockage effect). The generally accepted rule of the thumb is that the area of the blocking obstacle projected in a plane perpendicular to the flow is less than 5% of the wind tunnel test section. However, the most cogent physical limitation is often represented by the scale at which it is possible to reproduce in the wind tunnel the target wind flow characteristics (see Section 3.4), which must be scaled in the same way as the model of the Cathedral. Finally, the model used is 65 cm long, 22.5 cm wide, 22 cm high (top of the roof), and the spire is 48 cm high.

The model has been conceived as rigid, as a Gothic cathedral is very massive and poorly deformable, hence no aeroelastic phenomena are to be expected.

2.1 Fabrication technology

The realization of the physical scale model of Notre Dame was conditioned by some technological requirements. First, in order to have reliable experimental results, the model

175 must reproduce the geometry of the Cathedral with a high fidelity. This is quite a hard
176 task for a building like a Gothic Cathedral, which has a complex form and is rich of
177 details, like pinnacles, sculptures, etc. Then, the model must be instrumented with a
178 large number of pressure taps, cf. Section 2.2, placed everywhere over the surface of the
179 model. For these reasons, the model was fabricated using the 3D-printing technology, that
180 enables manufacturing possibilities which cannot be achieved through classical processes,
181 cf., e.g., [Ngo et al. \(2018\)](#), [Wang et al. \(2017\)](#), [Mitchell et al. \(2018\)](#), [Cano-Vicent et al.](#)
182 [\(2021\)](#). In particular, it is possible to realize objects not only with very complex shapes,
183 but also composed of different materials. Due to the dimensions and the geometrical
184 complexity of the Notre Dame Cathedral model, the FDM (Fused Deposition Modeling)
185 technology was chosen, except for those regions of the Cathedral characterized by very fine
186 details, e.g., the spire, manufactured via the SLA printing technology (stereolithography)
187 and assembled afterwards.

188 2.2 Model preparation, fabrication and materials

189 The model of the Cathedral has been fabricated starting from an existing high-fidelity
190 numerical mock-up ([MiniWorld3D 2019](#)). However, the numerical model has been thor-
191 oughly modified in order to obtain a physical model of the Cathedral at the scale of 1:200
192 well adapted to the wind tunnel tests, and to comply with the specificity of the FDM
193 printing technology. In fact, the physical model had to be equipped with many pressure
194 captors and it had to allow the different manipulations needed in the laboratory for the
195 set up of the experiment. Also, some modifications have been done on the original nu-
196 merical model in order to minimize the volume of material and the printing time. The 3D
197 computer graphics software Blender ([Blender Online Community 2021](#)), has been used to

198 work on the numerical model of the Cathedral.

199 The modifications have been carried out directly on the STL (Standard Tessellation
200 Language) file by means of boolean operations or via adjustments of the initial mesh. In
201 order to be able to place all of the 1200 flexible tubes that connect the holes on the model
202 surface to the pressure sensors, the walls of the model have been modified on the internal
203 side through the subtraction of a cone, so as to be possible to place the tubes in the holes.
204 This rather complicated operation has been made on the numerical model using a python
205 script coupled with Blender, modifying the file by some boolean operations. **The holes
206 for the pressure taps have also been printed, though in a second moment these have been
207 rectified with a mini-drill in the wind tunnel.**

208 The spire, which is rich in extremely fine details, has been fabricated using a more
209 precise numerical model ([3D Warehouse 2014](#)), and a 3D printer based upon the SLA
210 technology, that allows to obtain extremely precise objects, also when of very complicated
211 shape. The model of the spire so obtained has then been assembled with the Cathedral.

212 The whole model, Cathedral plus spire, is composed of 15 parts, separately fabricated
213 and then assembled together. This has been done for two reasons: the limits of the
214 printers (maximum height: 600 mm; maximum width: 390 mm) and the need of working
215 on the model for installing the many pressure captors. The different parts have been
216 assembled using magnets and bolts. A scheme of the parts of the model, some details of
217 it, showing also the holes for the captors, and the final physical model are shown in Fig. 2.

218 The 3D printing of the Cathedral mock-up was performed at the ENSAM facilities
219 in Bordeaux by means of a Lynxter S600D 3D printer ([Lynxter 2021](#)), equipped with a
220 single extrusion filament tool-head, selected in the light of its large building volume and
221 its excellent printing performance.

222 The 3D printing made use of white PolyMax™PLA filament that, thanks to its nano-
223 reinforcement technology, represents a suitable compromise between ease and quality of
224 printing and acceptable mechanical stiffness. The Simplify3D slicing software (Simplify3D
225 2021), was used to prepare the G-code files used by the printing machine. The total
226 printing time was about two weeks.

227 **2.3 The surrounding environment**

228 The mock-up of the buildings constituting the surrounding of the Cathedral has been
229 obtained by combining data from two sources: an existing STL file of the center of Paris,
230 cf. the website 3D CAD browser (2021), and 3D data extracted from the OpenStreetMap
231 database (OpenStreetMap 2017).

232 For the purposes of the wind tunnel tests, it was sufficient to realize buildings having
233 simplified shapes but correct (scaled) heights. The blocks of buildings constituting the
234 surrounding model are shown in Fig. 3(a).

235 Because of the significant total volume of the buildings and their simple shapes, the
236 model of the surrounding has been fabricated using wood plates, through a milling ma-
237 chine used to cut plates complying with the planforms of the buildings. An example of a
238 planform of an array of buildings is shown in Fig. 3(b). For a generic building, the final
239 height was obtained by simply stacking up and gluing together the milled wood plates.

240 Finally, the wind tunnel floor was lifted up of 4 cm, so to simulate the presence of
241 the Seine River, being the distance between the base of the Cathedral and the average
242 water level about 8 m at full scale. A view of the complete test set-up, with the models
243 of the Cathedral and the surrounding on the turning table of the wind tunnel is shown in
244 Fig. 3(c).

245 **3 Experimental campaign**

246 **3.1 General outline**

247 To determine the wind pressure field over the whole external surface of the Cathedral,
248 the physical model of Notre Dame has been equipped with 1200 pressure gauges, whose
249 distribution has been studied in order to obtain, by interpolation methods, detailed charts
250 of the pressure coefficients, cf. Section 4. As previously said, the study has been conducted
251 on the Cathedral model with and without the surrounding parts of Paris, see Fig. 4.
252 This, for two reasons: on the one hand, to evaluate the influence of the surrounding
253 buildings and, on the other hand, for obtaining pressure coefficient distributions that can
254 represent the wind loading on similar buildings immersed in a generic urban wind profile
255 (considering Notre Dame as a sort of Gothic Cathedral archetype). In both cases, the
256 wind profile has been generated through artificial roughness elements, cf. Section 3.4. The
257 test campaign has been carried out recording the pressure on the surface of the Cathedral
258 for many different wind directions, according to the scheme presented in Fig. 5. Therein,
259 the orientation of the Cathedral with respect to the canonical geographical directions, the
260 wind tunnel azimuths and the surrounding buildings can be seen. The direction denoted
261 as 0° (West-Northwest) is perpendicular to the main façade, while 90° means that the
262 wind blows perpendicularly to the naves from the side where the neighboring buildings
263 are closer to the Cathedral (North-Northeast). A wind direction of 270° indicates a wind
264 perpendicular to the naves but coming from the South-Southwest side.

265 **3.2 Wind tunnel facility**

266 The tests were carried out in the open-circuit boundary layer wind tunnel of CRIACIV² in
267 Prato, Italy. The facility is 22 m long and presents at the inlet a nozzle with a contraction
268 ratio of 3 to 1 after the honeycomb and a T-diffuser at the outlet. The test chamber is
269 1.6 m high, while the width varies from 2.2 m after the nozzle to 2.4 m at the position
270 of the turning table. The latter has a diameter of 2.2 m. The overall length of the fetch
271 to develop boundary layer flows is about 11 m. Air is drawn by a motor with a nominal
272 power of 156 kW, and the flow speed can be varied continuously up to about 30 m/s by
273 adjusting through an inverter the rotation speed of the fan or the pitch of its ten blades.
274 In the absence of turbulence generating devices, the free-stream turbulence intensity is
275 less than 1%.

276 **3.3 Model equipment**

277 The model of the Cathedral has been equipped with Teflon tubes with an internal diameter
278 of 1 mm, used to connect the taps on the model surface with the pressure sensors, see
279 Fig. 6. The tubes were 30 cm long, obtained by linking two pieces having the same
280 internal diameter with a short restrictor tube of about 1 cm working as a damper (see
281 e.g. Irwin et al. (1979)). Such pneumatic connections have been calibrated beforehand
282 to guarantee an acceptably flat transfer function in the frequency range of interest (up to
283 about 200 Hz in the present case) (see e.g. Holmes (2007)).

284 **Due to the limited number of pressure sensors available, groups of 222 pressure taps**
285 **were simultaneously recorded at a sampling rate of 500 Hz with the system PSI DTC**

²Centro di Ricerca Interuniversitario di Aerodinamica delle Costruzioni e Ingegneria del Vento, Inter-
University Research Centre on Building Aerodynamics and Wind Engineering

286 Initium. The restriction on the number of simultaneous signals logged is not an issue
287 if the mean pressures are concerned, but it must be borne in mind if the resultant load
288 on specific parts of the structure is calculated; indeed, the partial correlation of pressure
289 fluctuations has to be taken into account in this case. For this reason, the groups of
290 pressure taps have been chosen based on the structural macro-elements of the Cathedral.
291 The accuracy of the piezoelectric sensors of the 32-port miniaturized ESP-32HD pressure
292 scanners is ± 2.45 Pa. Each signal was recorded for about 120 s at a reference mean wind
293 speed of about 19.5 m/s at the top of the Cathedral roof.

294 At full scale, following the Eurocode 1 (CEN 2004), a mean wind speed of 21.3 m/s is
295 expected at a height of 44 m (top of the roof) for a terrain category IV (urban profile) and a
296 return period of 50 years. Consequently, the velocity scale of the tests is about 1:1.1, while
297 the time scale results to be about 1:183. This means that a sampling frequency of 500 Hz
298 allows detecting pressure fluctuations at full scale up to a frequency of about 1.37 Hz, thus
299 encompassing the most energetic atmospheric turbulent fluctuations. Moreover, 120 s at
300 laboratory scale correspond to 21960 s at full scale, that is more than 36 time windows of
301 10 minutes, which is suitable to calculate the statistics of the peak values of pressures in
302 compliance with Eurocode 1 (see also Section 4.2).

303 3.4 Oncoming flow

304 For the city centre of Paris, the previously mentioned turbulent wind profile associated
305 with the terrain category IV of Eurocode 1 has been assumed for all azimuthal directions.
306 The atmospheric boundary layer flow at the same scale of the model (1:200) has been
307 reproduced through artificial roughness elements of variable size diffused all over the floor
308 of the test chamber. A castellated barrier, placed at the inlet section of the wind tunnel

309 has also been employed to increase the turbulence intensity.

310 Fig. 7 shows the modeled wind characteristics in the wind tunnel at the beginning
311 of the turning table, slightly upstream of the model of the Cathedral. Flow velocity
312 measurements were carried out with a single-component hot-wire anemometer recorded at
313 a sampling rate of 10 kHz. The mean wind velocity pattern is in very good agreement with
314 the assumed target urban profile (Fig. 7(a)). The longitudinal turbulence intensity, which
315 is a normalized integral measure of the wind velocity fluctuations (a coefficient of variation,
316 indeed), is slightly lower than the Eurocode 1 target (Fig. 7(b)). The longitudinal integral
317 length scale of turbulence, which represents the correlation length of the wind velocity
318 fluctuations along the mean velocity direction and rules the frequency distribution of the
319 turbulent kinetic energy in the stream (see e.g. Simiu and Yeo (2019)), closely follows the
320 target pattern up to about 30 m above the ground; afterwards, the increase with the height
321 becomes slower than in the Eurocode 1 profile (Fig. 7(b)). However, the discrepancy is
322 moderate at least up to the top of the Cathedral roof. Finally, Fig. 7(d) shows that
323 the spectral characteristics of the generated boundary layer comply very well with a von
324 Kármán-Harris spectrum, which is very often assumed to describe the energy cascade of
325 turbulence, Simiu and Yeo (2019). Measurements have also been carried out to assess the
326 homogeneity of the flow in the transversal and longitudinal directions.

327 In general, despite the large scale of the model with respect to the present wind tunnel
328 facility, we can conclude that the modeled turbulent wind is well representative of an urban
329 environment such as the one that can be expected in the centre of Paris.

330 As said above, two different configurations of the model have been tested. In the
331 first one, the turning table was covered with roughness elements of progressively reduced
332 height close to the Cathedral model (cf. Fig. 4(a)), in order to transfer the same generic

333 urban wind profile from the beginning of the turning table to the model position and
334 beyond. In contrast, the second configuration includes the model of the surrounding of
335 the Cathedral, as shown in Fig. 4(b).

336 4 Results of the experimental tests

337 The results of pressure measurements on the external surface of the Cathedral are reported
338 in this section in the form of pressure coefficients, defined as follows:

$$C_p = \frac{p - p_0}{\frac{1}{2}\rho V^2(z_{ref})}, \quad (1)$$

339 where p is the pressure on the considered point of the structure, p_0 is the static pressure
340 of the undisturbed flow in the wind tunnel at the position of the model, ρ is the air
341 density and $V(z_{ref})$ is the reference wind speed, that is the mean flow velocity at the top
342 of the roof ($z_{ref} = H = 44$ m at full scale) in the absence of the model (see the mean
343 wind velocity profile in Fig. 7(a)). It is noteworthy that the accuracy of the pressure
344 transducers, given the reference velocity pressure in the tests, corresponds to ± 0.01 in
345 terms of C_p . The recorded data can be divided in mean pressure and gust pressure data.
346 The former are simply calculated as the time averages of the recorded pressure coefficients.
347 The latter are defined as the average of either the maximum or the minimum values of
348 C_p registered over full-scale time windows of 10 minutes (see Section 4.2). The results are
349 reported hereafter in terms of pressure coefficient charts, obtained by linear interpolation
350 and heuristically controlled extrapolation of the measured values. The small black spots
351 indicate the taps where pressure was actually measured.

352 4.1 Mean pressure charts

353 Fig. 8 gives the global distribution of the pressure coefficients on the lateral side of the
354 Cathedral in the presence of the surrounding model and wind coming from the 90°-
355 direction. It is worth noting the strong pressure gradient in correspondence of the wind-
356 ward rose of the transept and the large pressure coefficients in the higher part of the
357 transept ($C_p > 0.9$).

358 The pressure coefficient distribution over the front of the Cathedral is reported in
359 Fig. 9 for a wind perpendicular to it (0°-direction). It is apparent that the particular
360 geometry of the towers produces large pressure gradients close to the edges of the façade.
361 It is also noteworthy that values of C_p larger than unity can be found in the upper part
362 of the towers; this is because the reference velocity pressure is taken at a lower height,
363 that is that of the top of the roof (see Eq. (1)).

364 Mean pressure coefficient charts are presented in Fig. 10 also for the apse, for a wind
365 blowing either from the direction perpendicular to the left flank (90°) or parallel to the
366 longitudinal axis of the Cathedral (180°). In the former case, one can notice a strong pres-
367 sure gradient due to the curvature of the walls, **which from positive pressure coefficients**
368 **around 0.35** on the windward side quickly leads to strong suction **(up to $C_p \cong -0.8$)** in
369 the middle upper part. In contrast, for a wind direction of 180° positive mean pressure
370 coefficients up to about 0.8 are attained in the central upper portion of the apse. In the
371 lower part of the left side of the apse (bottom right corner in Fig. 10(a) and 10(b)), one
372 can also remark the effect of the surrounding buildings, which are very close to the apse.
373 They shelter the flank of the Cathedral from direct wind for an azimuth angle of 90°,
374 while they promote a flow acceleration, and then a pressure decrease, for a wind direction
375 of 180°.

376 4.1.1 Detail of the flank

377 A lateral portion of the Cathedral between the front and the transept (indicated in red in
378 Fig. 5) has been very densely instrumented, in order to have more details of the pressure
379 coefficient distribution through the height of the Cathedral on a representative part of
380 it. Results are shown in Fig. 11. In the case of a generic urban profile (i.e., without
381 surrounding, Fig. 11(a)), pressure coefficients between about 0.6 and 0.75 are found on the
382 windward walls. However, the most interesting features can be observed on the windward
383 side of the roof, where a bubble of high pressure (with mean pressure coefficients up to
384 about 0.55) is apparent in the central part. This is due to the flow acceleration on the
385 upper side of the roof (with consequent decrease of pressure) and the strong inclination of
386 the flow that locally separates at the balustrade at the base of the roof. Flow visualizations
387 with a smoke generator (Fig. 12) revealed that this is also due to the significant vertical
388 wind component induced by the three orders of walls on the flank of the Cathedral. On
389 the leeward side, the pressure is nearly uniform, with mean C_p values between about
390 -0.45 and -0.4 .

391 Fig. 11 clearly shows how the presence of the buildings upstream of the Cathedral and
392 very close to it affects the load distribution. The pressure remarkably decreases on the
393 lower part of the windward walls **due to the sheltering effect of the neighboring buildings**
394 **(in some regions, the pressure coefficients even pass from about 0.6 to about 0.2)**, but the
395 vertical wind velocity component also reduces, producing a slight increase of the mean
396 C_p on the upper portion of the windward wall and a pronounced increment on the roof
397 **(of the order of 20-25% but even higher at the base of the roof, behind or just above the**
398 **balustrade)**. **An increase of pressure between about 10 and 25%** can also be observed on
399 the leeward side of the Cathedral (lower suction).

400 4.1.2 Roof

401 The results discussed in the previous section are confirmed by Fig. 13, which reports the
402 pressure distribution on the entire roof of the Cathedral. It can be remarked that, despite
403 the roof is at a significantly greater height than the surrounding buildings, the presence
404 of the latter has a remarkable impact on the pressure distribution over it, as previously
405 said, probably accelerating the upper flow and reducing the vertical component of the
406 velocity with which the wind attacks the windward pitch of the roof. Indeed, while the
407 pressure coefficient hardly attains 0.57 in a small windward region between the façade
408 and the transept when the surrounding buildings are not reproduced, it overcomes 0.7 at
409 several locations if the latter are in place.

410 4.2 Peak loads

411 For the local design or verification of cladding elements or secondary structures, and also
412 to have a statistical measure of the fluctuation of pressures, peak values can be calculated
413 according to Davenport (1961)'s approach, i.e. as the average of maxima (or minima)
414 associated with a given observation time (600 s according to Eurocode 1's approach).
415 Given the time scale of the current experiments, as said in Section 3.3, the length of
416 the recorded signals corresponds to about 36 windows of 10 minutes at full scale and
417 allows a statistically meaningful calculation of wind load peak values. Moreover, to be
418 representative of area-averaged pressures, the maxima (or minima) are calculated on time
419 records filtered via a moving average over a set time window (Lawson 1976, Holmes 1997).
420 In the present analysis, the classical full-scale window of 1 s has been chosen.

421 Fig. 14 shows the distribution of the maximum pressure coefficients on the North-
422 Northeast flank of the Cathedral for a wind perpendicular to the walls (90°-direction).

423 Large values of the load can be observed due to wind gusts, the C_p chart showing values
424 even beyond 2. The higher peak pressures are obtained just above the big rose window
425 of the transept façade. The comparison with Fig. 8(a) shows that high gust factors (ratio
426 of maximum to mean value of pressures) mostly between about 2.4 and 4 are obtained.

427 The comparison of Fig. 14(a) and Fig. 14(b) emphasizes the effect of the surrounding
428 buildings around the Cathedral on the peak pressure coefficients. Coherently with the
429 observations already done for the mean pressures (see Figs. 10 and 11, and Sections 4.1.1-
430 4.1.2), the presence of the surrounding strongly reduces the peak pressure coefficients
431 on the lower part of the Cathedral flank (with decrements of about 50 to 70%), slightly
432 increases them (up to about 10%) in the upper part of the lateral walls and on the transept
433 façade, and remarkably intensifies the load on the roof (+15 to 25% in the central band).

434 Though not reported in Fig. 14, it is worth noting that the pressure fluctuations are
435 such that the minimum coefficients on the windward side of the Cathedral often reach
436 negative values (nearly everywhere in the configuration with surrounding buildings).

437 Given the possible vulnerability of large Gothic rose window, as highlighted by Sois-
438 sons's recent disaster mentioned in the Introduction, the pressures acting on the great
439 roses of the transept have been integrated at each time instant to account for the non-
440 perfect simultaneity of the fluctuations, thus estimating a resulting force coefficient C_D .
441 The center of the rose windows is at a height above the ground of 25.8 m, and these
442 have a surface area of about 85 m². A specific set of measurements has been used to this
443 purpose, where the two facades of the transept are finely instrumented. Specifically, the
444 pressure field on the rose windows is discretized with 30 pressure taps. The resulting time
445 histories are shown in Fig. 15 for the wind directions perpendicular to the transept façade
446 (90° and 270°). It is apparent that the maximum load is obtained in the case without

447 surrounding for the windward window (Fig. 15(a); the nondimensional mean thrust is
448 0.82, while the peak value is 2.17). The load reduces by about 40% when the surrounding
449 portion of the city is modeled and the wind blows from North-Northeast (Fig. 15(c), 90°-
450 wind direction), due to the sheltering effect of the buildings very close to the Cathedral.
451 Nevertheless, the load reduction is only 13% when the wind comes from South-Southwest
452 (Fig. 15(d), 270°-wind direction) due to larger distance of the surrounding buildings. The
453 leeward window is less loaded, and the resulting mean suction in the presence of the sur-
454 rounding model is nearly the same as without surrounding (Fig. 15(b)) for the 270°-wind
455 direction ($\bar{C}_D = -0.43$), while a remarkable reduction is observed for the 90°-wind direc-
456 tion ($\bar{C}_D = -0.34$). On the other hand, on the windward rose window load fluctuation
457 increases in the presence of the surrounding model, and the peak force even becomes the
458 same as in the case of a generic urban wind profile for a wind direction of 270° (Fig. 15(d),
459 $C_{D,max} = 2.15$).

460 5 Discussion

461 5.1 General considerations

462 The results reported in the previous section revealed that the Cathedral's geometrical
463 complexity reflects on the measured pressure field. Apart from the remarkable peculiarity
464 of the apse and the main façade of the Cathedral, for the sake of simplification one may
465 say that the Cathedral of Notre Dame is a long construction with a depth discontinuously
466 varying with the height (see the schematics in Fig. 16), so that the height-to-depth ratio is
467 small (close to 1) considering the lower part of the church but significantly higher (about
468 2.3) referring to the top of the vertical walls. Also, the roof presents a high pitch (about

469 55°), and there are several other architectural elements (such as the jutting out body of
470 the transept, the large flying buttresses, the balustrade at the base of the roof, or the
471 various orders of gables) that are supposed to significantly influence the aerodynamic
472 behavior of the construction. It is clear that the urban integration of the structure also
473 plays a key role.

474 From the practical engineering standpoint, however, it is important to understand
475 if all the specific aerodynamic features of a large Gothic Cathedral lead to significantly
476 different wind loads for design or safety verification purposes compared to a more-or-less
477 ordinary building. It is also to be noticed that only canonical wind velocity directions have
478 been analyzed so far (those parallel or perpendicular to the Cathedral’s symmetry plane),
479 while all possible wind directions must be considered instead for engineering purposes.
480 Bearing in mind all these aspects, in the next section the load envelopes obtained for the
481 finely-instrumented representative portion of the flank of the Cathedral (see Section 4.1.1)
482 are compared with the few data available in the literature and with the loads proposed
483 by Eurocode 1 for standard buildings.

484 **5.2 Comparison with load models available in the literature**

485 The mean pressure coefficients obtained for the finely instrumented portion of the flank
486 of the Cathedral and the roof (Section 4.1.1) were averaged along the direction parallel
487 to the longitudinal axis of the Cathedral (i.e., along the width of the considered Cathe-
488 dral “slice”). Moreover, to comply with the prescriptions of Eurocode 1 (CEN 2004), the
489 envelope pressure coefficients were calculated at any height above the ground for wind
490 azimuths between -45° and $+45^\circ$ around the direction perpendicular to one of the Cathe-
491 dral’s flanks. Results are reported in Fig. 16. It is noteworthy that, in the case of a generic

492 urban wind profile (without surrounding), the maximum mean pressure coefficient on the
493 windward side is obtained for small or null skewness of the wind direction with respect to
494 the canonical azimuths (either 90° or 270°); therefore, the results for a wind perpendicular
495 to the lateral walls represent a good estimate of the worst load case. In contrast, for the
496 leeward side, the canonical wind directions provide nearly the lower load, whereas the
497 higher suctions are obtained for inclinations of about 45° with respect to them. Clearly,
498 results are more complicated and rather different for two flanks of the Cathedral when
499 the surrounding buildings are modeled.

500 The comparison of the results for the configurations with and without surrounding
501 emphasizes the importance of modeling the buildings, the river and the other details
502 of the city around the Cathedral. As expected, for the case without surrounding, both
503 windward and leeward pressure coefficient envelopes on the right and left sides of the
504 Cathedral are nearly identical. On the windward side, in the presence of the surrounding
505 model, the pressure coefficient envelope exhibits significantly lower values in the inferior
506 part of the walls (with reductions up to about 60-70%) when one considers the left flank of
507 the Cathedral (then, when the wind direction is between 45° and 135° , and the buildings
508 are close to the church; see Fig. 5). In contrast, on the right flank (then, if the wind
509 blows from directions 225° and 315°), the pressure coefficients are very similar to the
510 case without surrounding in the lower part of the walls. For a height above the ground
511 between about $0.6H$ and $0.75H$, the windward pressure envelopes for the left and right
512 flanks of the Cathedral become fairly close and non-negligibly higher than the case without
513 surrounding (with increments up to nearly 20%). As for the leeward pressure coefficient
514 envelopes, the suction is lower if the surrounding buildings are modeled; in particular,
515 the difference is on average of 12 and 17% for the left and right side of the Cathedral,

516 respectively.

517 The measured pressure coefficients on the windward side of the considered part of
518 the Cathedral are generally lower (or even much lower in some regions) than the values
519 suggested by Eurocode 1, except for a small portion of the roof for the case with sur-
520 rounding. In contrast, on the leeward side the measured pressures tend to be slightly
521 lower (higher suction) on the vertical walls of the Cathedral and significantly lower on
522 the roof, especially for the configuration without surrounding. In particular, for a generic
523 urban boundary layer flow, the integral mean normal force coefficient acting on the wind-
524 ward side of the roof results to be more than 30% lower than Eurocode 1's prescriptions,
525 whereas that acting on the leeward side is more than double. Consequently, both the
526 resulting drag and uplifting forces are increased. The same effects are also observed if
527 the buildings surrounding the Cathedral are modeled, but the decrease/increase of the
528 windward/leeward normalized forces are less pronounced. Finally, the experimental data
529 by Mark and Jonash (1970) for a Cathedral-like construction are in agreement with the
530 pressure coefficient envelopes in the lower part of the windward vertical walls for the case
531 of a generic urban boundary layer, while they overestimate the loads in the upper part.
532 In contrast, on the leeward side these literature data underestimate the suction on most
533 part of the vertical walls, but they overestimate it in the top part.

534 Considering again the large roses of the transept (see Fig. 15), one can remark that the
535 mean load without surrounding on the windward window is in line with the prescriptions
536 of Eurocode 1 (Fig. 16), provided that the velocity pressure at the top of the roof is used to
537 normalize the force or the pressure coefficient (which is not the only option in Eurocode 1).
538 The gust factor (ratio of peak to mean load) for the windward rose perfectly complies
539 with the value suggested by Eurocode 1 (slightly less than 2.2) based on the turbulence

540 intensity in the approaching wind profile at the height of the window. In contrast, it is
541 higher in the presence of the surrounding buildings (larger than 3). However, it is very
542 important to stress that the canonical wind directions (either 90° or 270°) considered in
543 the analysis of the load on the rose windows (see Fig. 15) do not always represent the
544 worst case scenario, especially for negative pressures on the leeward side, as it has already
545 been emphasized for the finely instrumented portion of the flank of the Cathedral. In
546 particular, mean suction forces as low as -0.63 (for a wind direction of either 135° or
547 225°) and -0.73 (for a wind direction of 130°) have been obtained for the cases without
548 and with surrounding, respectively.

549 Finally, one can notice that the effective load acting on most parts of the Cathedral
550 will also depend on the internal pressures, which have not been investigated in the present
551 work. Their estimation is a very complicated task as it requires the accurate modeling
552 of diffused openings all over the building. However, in the absence of dominant openings
553 (produced, for instance, by the failure of a window), for structural verifications it may
554 be reasonable to consider the standard range -0.3 to $+0.2$ recommended by Eurocode 1
555 (CEN 2004).

556 6 Conclusions

557 The results of the wide wind tunnel test campaign that has been carried out on a scale
558 model of the Cathedral of Notre Dame in Paris led to some major conclusions, reported
559 hereafter.

560 Firstly, the complex geometry of a large Gothic cathedral, both in the aerial projection
561 and in elevation, as well as the important aerodynamic role played by some architectural
562 elements imply specific phenomena in the wind-structure interaction process that do not

563 allow the correct estimation of the wind loads based on the data available for standard
564 buildings. Specifically, the present results reveal that, depending on the structural element
565 considered or the specific configuration examined, these loads can be either significantly
566 higher or lower than the values that can be predicted based on codes and standards.
567 In particular, the roof of the Cathedral may be subjected to drag and uplifting forces
568 significantly larger than those calculated with the Eurocode 1, which demonstrates the
569 need for accurate wind tunnel tests to assess the safety of this type of structures.

570 Secondly, the influence on the wind load of the neighboring portion of the city where
571 the considered Cathedral stands is extremely important, and can vary on a case-by-case
572 basis. The current analysis highlights that the presence of the surrounding buildings
573 does not only affect the aerodynamics of the portions of the Cathedral at a comparable
574 height but also of parts significantly above. For instance, the drag force on the roof of
575 the Cathedral increases by nearly 10%, while the uplifting force reduces to about one
576 third. For the large rose windows of the transept, another potentially sensitive element of
577 the Cathedral, the behavior is more complicated; indeed, the modeling of the neighboring
578 portion of the city implies a lower mean thrust force but also a rise of the load fluctuations.

579 The results reported in the current paper may represent a guideline to determine the
580 wind load on complex buildings such as Gothic Cathedrals. Nevertheless, once the wind
581 climate in the city of Paris has accurately been evaluated, the nondimensional pressure
582 coefficients presented herein can be transformed in loads and used to assess the structural
583 safety of the Cathedral of Notre Dame, in a similar way to the analysis carried out by
584 Vannucci et al. (2019). Therefore, this work may represent a first step towards the goal
585 of guaranteeing the wind safety of architectural treasures like Gothic Cathedrals, even if
586 in the future heavier and heavier effects of climate change are likely to occur.

587 Acknowledgments

588 Authors want to thank:

- 589 • Martin Peters, former director of the Eiffel Wind Tunnel Laboratory, Paris, for his
590 valuable help concerning the history of wind tunnel research on historical monu-
591 ments.
- 592 • Emmanuel Portet and Laure Frèrejean, University of Versailles and Saint Quentin,
593 for their fruitful commitment and help in the administrative and financial aspects
594 of this research.
- 595 • Bernardo Nicese, Clara Gessl and Petar Melnjak, who helped us in the execution of
596 the laboratory tests in Prato.

597 References

- 598 3D CAD browser (2021). www.3dcadbrowser.com.
- 599 3D Warehouse (2014). Notre Dame de Paris.
600 <https://3dwarehouse.sketchup.com/model/cf5038cd918ff49c63995fb119e59971/Notre->
601 Dame-de-Paris.
- 602 Blender Online Community (2021). *Blender - a 3D modelling and rendering package*
603 *(release 3.0)*. Stichting Blender Foundation, Amsterdam: Blender Foundation.
- 604 Blocken, B. (2014). 50 years of computational wind engineering: Past, present and future.
605 *Journal of Wind Engineering and Industrial Aerodynamics* 129, 69–102.
- 606 Borri, C. and L. Facchini (1999). Wind induced loads on the monumental roof structure of
607 the XII century, Palazzo della Ragione, in Padova. In *Proc. of 10th ICWE (International*

608 *Conference on Wind Engineering*), *Copenhagen*, Volume II, Rotterdam, Denmark, pp.
609 1105–1111. Balkema A. A.

610 Brocato, M., I. Stefanou, P. Vannucci, C. Coulangeon, M. Ferrucci, F. Pantalone, E. De-
611 chorgnat, F. Oran, A. Pallard, J. Pellerin, A. Diao, M. Kun, and A. A. Albero (2016).
612 AVACAT, Analyse de vulnérabilité de l’architecture capétienne face aux tempêtes.
613 Technical report, ENSA Paris-Malaquais, Laboratoire GSA.

614 Calderini, C. and L. C. Pagnini (2015). The debate on the strengthening of two slen-
615 der masonry structures in early xx century: A contribution to the history of wind
616 engineering. *Journal of Wind Engineering and Industrial Aerodynamics* 147, 302–319.

617 Cano-Vicent, A., M. M. Tambuwala, S. S. Hassan, D. Barh, A. A. A. Aljabali, M. Birkett,
618 A. Arjunan, and A. Serrano-Aroca (2021). Fused deposition modelling: Current status,
619 methodology, applications and future prospects. *Additive Manufacturing* 47, 102378.

620 CEN, E. C. f. S. (2004). EN 1991-1-4, Eurocode 1: Part 4: wind actions.

621 Chien, N., Y. Feng, H. H. Want, and T. T. Siao (1951). Wind tunnel studies of pressure
622 distribution on elementary building forms. Technical report, Institute of Hydraulics
623 Research, University of Iowa, Ames, Iowa.

624 Coccia, S., M. Como, and F. D. Carlo (2015). Wind strength of Gothic Cathedrals.
625 *Engineering Failure Analysis* 55, 1–25.

626 Como, M. (2013). *Statics of historic masonry constructions*. Berlin, Germany: Springer
627 Verlag.

628 Davenport, A. G. (1961). The application of statistical concepts to the wind loading of
629 structures. *Proceedings of the Institution of Civil Engineers* 19(4), 449–472.

- 630 Deland, T. T., M. Sadegh, and K. T. Sina (2020). The semantic conservation of architec-
631 tural heritage: the missing values. *Heritage Science* 8, 70.
- 632 Domede, N., L. Pena, and N. Fady (2019). Historical review of lighthouse design under
633 wind load: the Ile Vierge lighthouse. *Philosophical Transactions of the Royal Society*
634 *A: Mathematical, Physical and Engineering Sciences* 377(2155), 20190167.
- 635 Ferrucci, M. and M. Peter (2020). La puissance de la recherche incosciente: cent ans
636 d'expérimentation aérodynamique à la soufflerie eiffel. In *Architecture et Expérimenta-*
637 *tion*, pp. 44–75. Rouen, France: ATE - Editions des Méandres.
- 638 Holmes, J. D. (1997). Equivalent time averaging in wind engineering. *Journal of Wind*
639 *Engineering and Industrial Aerodynamics* 72, 411–419.
- 640 Holmes, J. D. (2007). *Wind Loading of Structures* (second ed.). CRC Press.
- 641 Irwin, H. P. A. H., K. R. Cooper, and R. Girard (1979). Correction of distortion ef-
642 fects caused by tubing systems in measurements of fluctuating pressures. *Journal of*
643 *Industrial Aerodynamics* 5, 93–107.
- 644 Lawson, T. V. (1976). The design of cladding. *Building and Environment* 11, 37–38.
- 645 Lynxter (2021). Industrial multi-materials 3D printer S600D.
646 <https://lynxter.fr/en/product/professional-industrial-3d-printers/>.
- 647 Mark, R. (1982). *Experiments in gothic structure*. Cambridge, Massachussets: MIT Press.
- 648 Mark, R. (1984). *High gothic structure - A technological reinterpretation*. Princeton, New
649 Jersey: Princeton University Press.
- 650 Mark, R. and R. S. Jonash (1970, 10). Wind Loading on Gothic Structure. *Journal of*
651 *the Society of Architectural Historians* 29(3), 222–230.

652 MiniWorld3D (2019). Notre-Dame de Paris Cathedral.
653 [https://www.myminifactory.com/object/3d-print-notre-dame-de-paris-cathedral-](https://www.myminifactory.com/object/3d-print-notre-dame-de-paris-cathedral-91899)
654 91899.

655 Mitchell, A., U. Lafont, M. Hołyńska, and C. Semprimoschnig (2018). Additive manufac-
656 turing — a review of 4d printing and future applications. *Additive Manufacturing* 24,
657 606–626.

658 Ngo, T. D., A. Kashani, G. Imbalzano, K. T. Nguyen, and D. Hui (2018). Additive man-
659 ufacturing (3d printing): A review of materials, methods, applications and challenges.
660 *Composites Part B: Engineering* 143, 172–196.

661 OpenStreetMap (2017). Map of Paris. <https://www.openstreetmap.org> .

662 Orr, S. A., J. Richards, and S. Fatorić (2021). Climate change and cultural heritage: A
663 systematic literature review (2016–2020). *The Historic Environment: Policy & Prac-*
664 *tice* 0(0), 1–43.

665 Romani, L. (1972). Rouen, Place du Vieux Marché, Efforts du vent sur l’église (mesures
666 en soufflerie). Technical report, Laboratoire Aérodynamique Eiffel.

667 Simiu, E. and D. Yeo (2019). *Wind Effects on Structures - Modern Structural Design for*
668 *Wind* (fourth ed.). Wiley Blackwell.

669 Simplify3D (2021). All-In-One 3D Printing Software - Simplify3D software.
670 <https://www.simplify3d.com/>.

671 Solari, G., T. A. Reinhold, and F. Livesey (1998). Investigation of wind actions and effects
672 on the Leaning Tower of Pisa. *Wind and Structures* 1(1), 1–23.

673 Steenbergen, R. D. J. M., T. Koster, and C. P. W. Geurts (2012). The effect of cli-
674 mate change and natural variability on wind loading values for buildings. *Building and*
675 *Environment* 55, 178–186.

676 Szalay, Z. (1983). Wind loads on an ancient church spire. *Journal of Wind Engineering*
677 *and Industrial Aerodynamics* 11(1), 187–199.

678 Ungewitter, G. G. (1890). *Lehrbuch der Gotischen Konstruktionen*. Leipzig, Germany.
679 Available at Biblioteca Meccanico Architettonica: <http://www.bma.arch.unige.it>: T.
680 O. Weigel Nachfolger.

681 Vannucci, P. (2021). A study on the structural functioning of the ancient charpente of
682 Notre-Dame, with a historical perspective. *Journal of Cultural Heritage* 49, 123–139.

683 Vannucci, P., F. Masi, and I. Stefanou (2019). A nonlinear approach to the wind strength
684 of Gothic Cathedrals: The case of Notre Dame of Paris. *Engineering Structures* 183,
685 860–873.

686 Wang, X., M. Jiang, Z. Zhou, J. Gou, and D. Hui (2017). 3D printing of polymer matrix
687 composites: A review and prospective. *Composites Part B: Engineering* 110, 442–458.

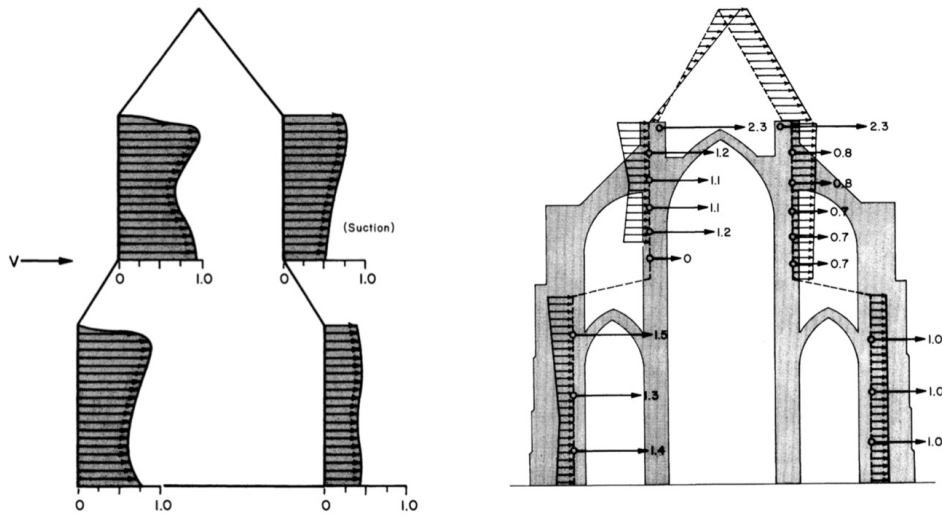


Figure 1: The wind pressure coefficients as experimentally measured in [Chien et al. \(1951\)](#), left, and how they are applied to a bi-dimensional Cathedral model in [Mark and Jonash \(1970\)](#), right.

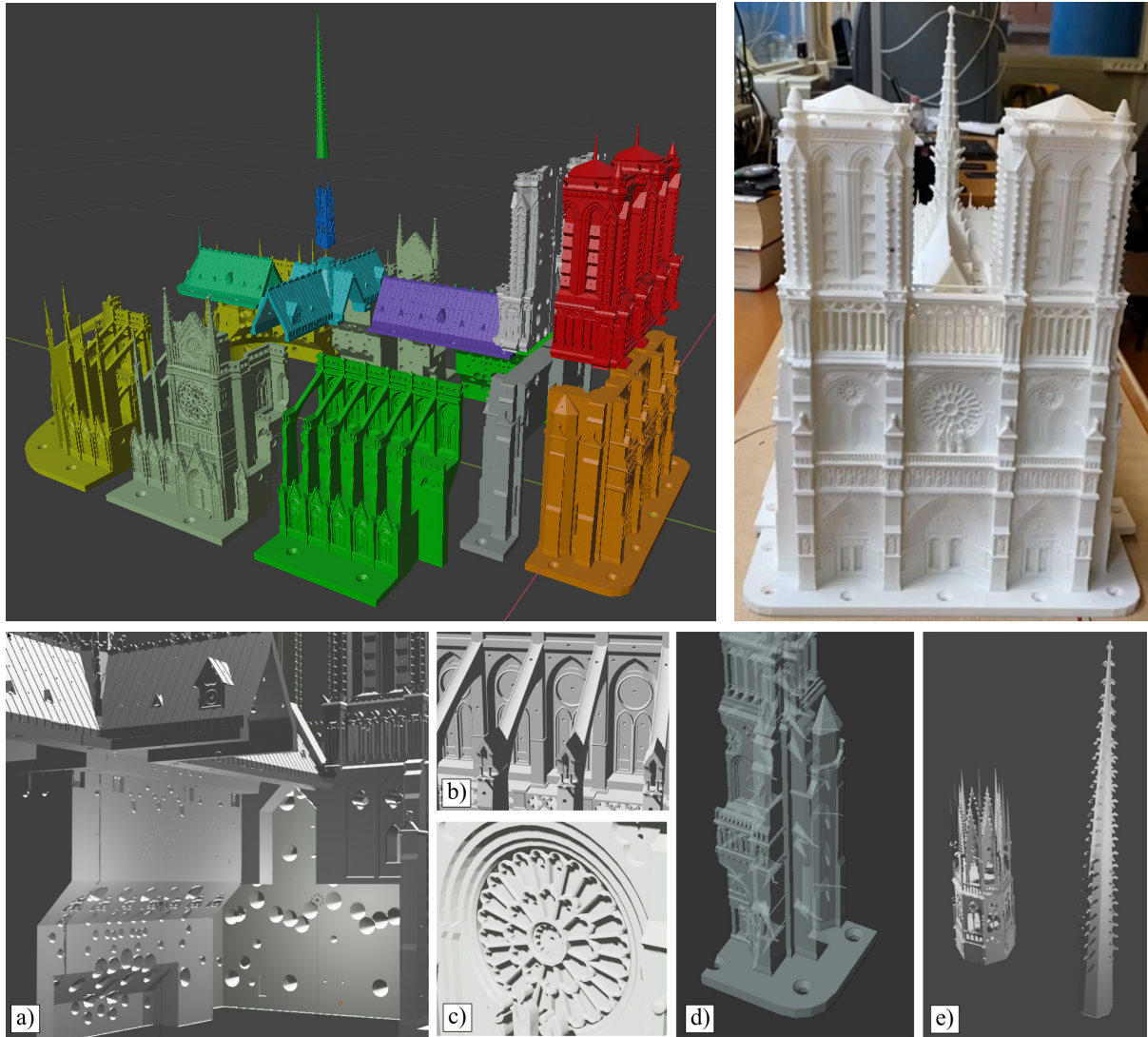


Figure 2: The Cathedral model: top, left: the 15 parts of the numerical model; right: the fabricated model; bottom: a) detail of the internal volume (façade and nave) with the conical holes to place the pressure tubes; b) detail of the external surface of the nave; c) detail of the rose on the façade; d) internal view of a portion of the façade; e) spire model split into two parts.

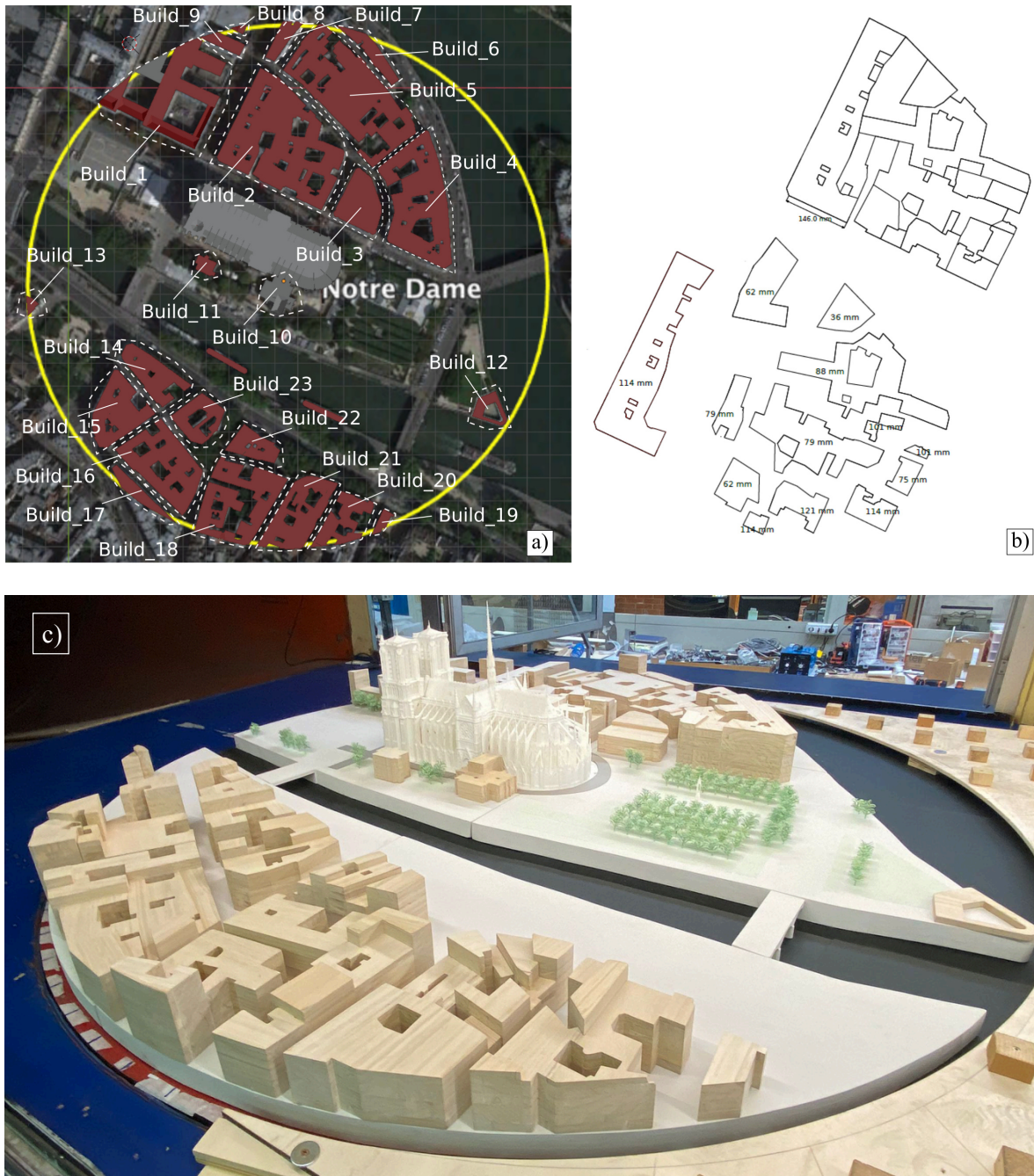


Figure 3: Model of the surrounding of the Cathedral; a) selected blocks of buildings for the model; b) example of a planform with the internal building partitions; c) view of surrounding and Cathedral models mounted on the turning table in the wind tunnel.

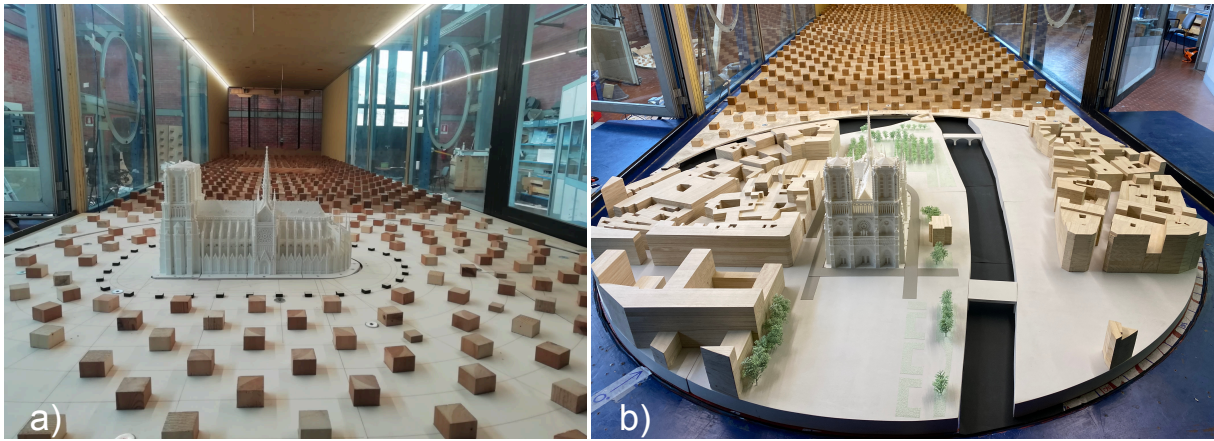


Figure 4: Model of the Cathedral in the wind tunnel: a) without and b) with surrounding.

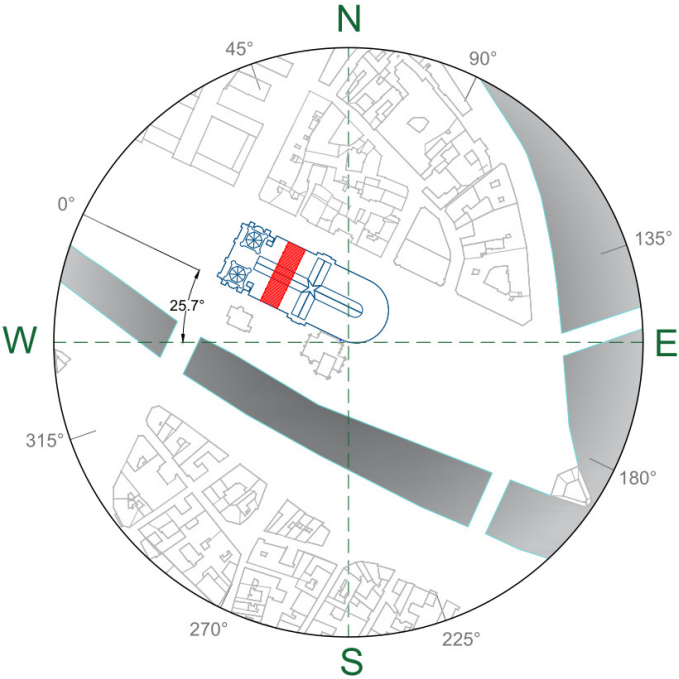


Figure 5: Scheme indicating the wind directions with respect to the Cathedral (the 0°-direction is perpendicular to the front of the building). The portion of the flank of the Cathedral that has been studied in detail in Section 4.1.1 is highlighted in red.



Figure 6: Parts of the model equipped with pressure taps; the Teflon tubes are connected to an ESP pressure scanner (the black box visible at the bottom).

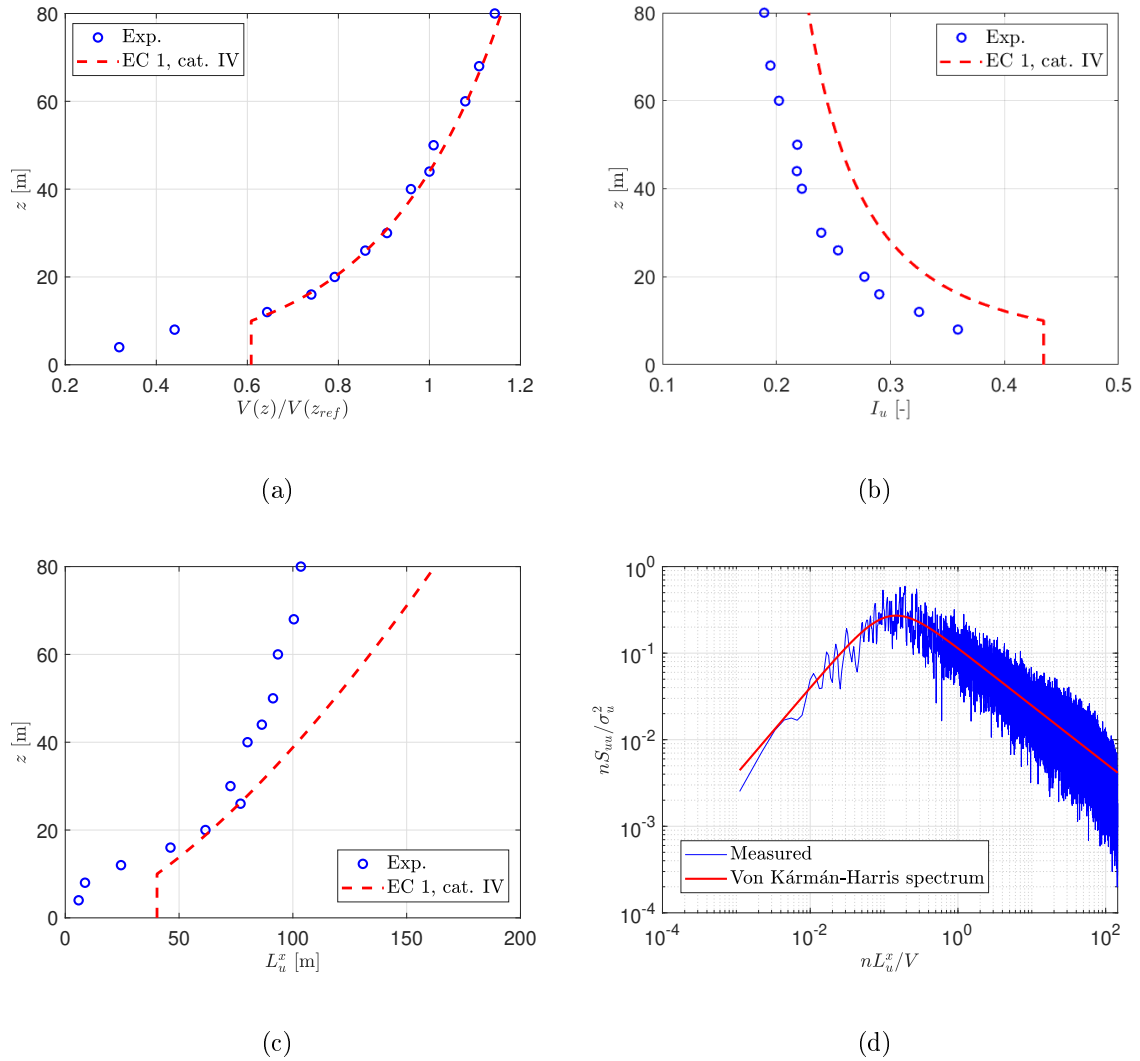


Figure 7: (a) Normalized mean velocity ($z_{ref} = H = 44$ m denotes the reference height, i.e., the top of the roof), (b) turbulence intensity, and (c) longitudinal integral length scale of turbulence profiles in the present tests. The power spectral density of longitudinal velocity fluctuations at the reference height is shown too (d).

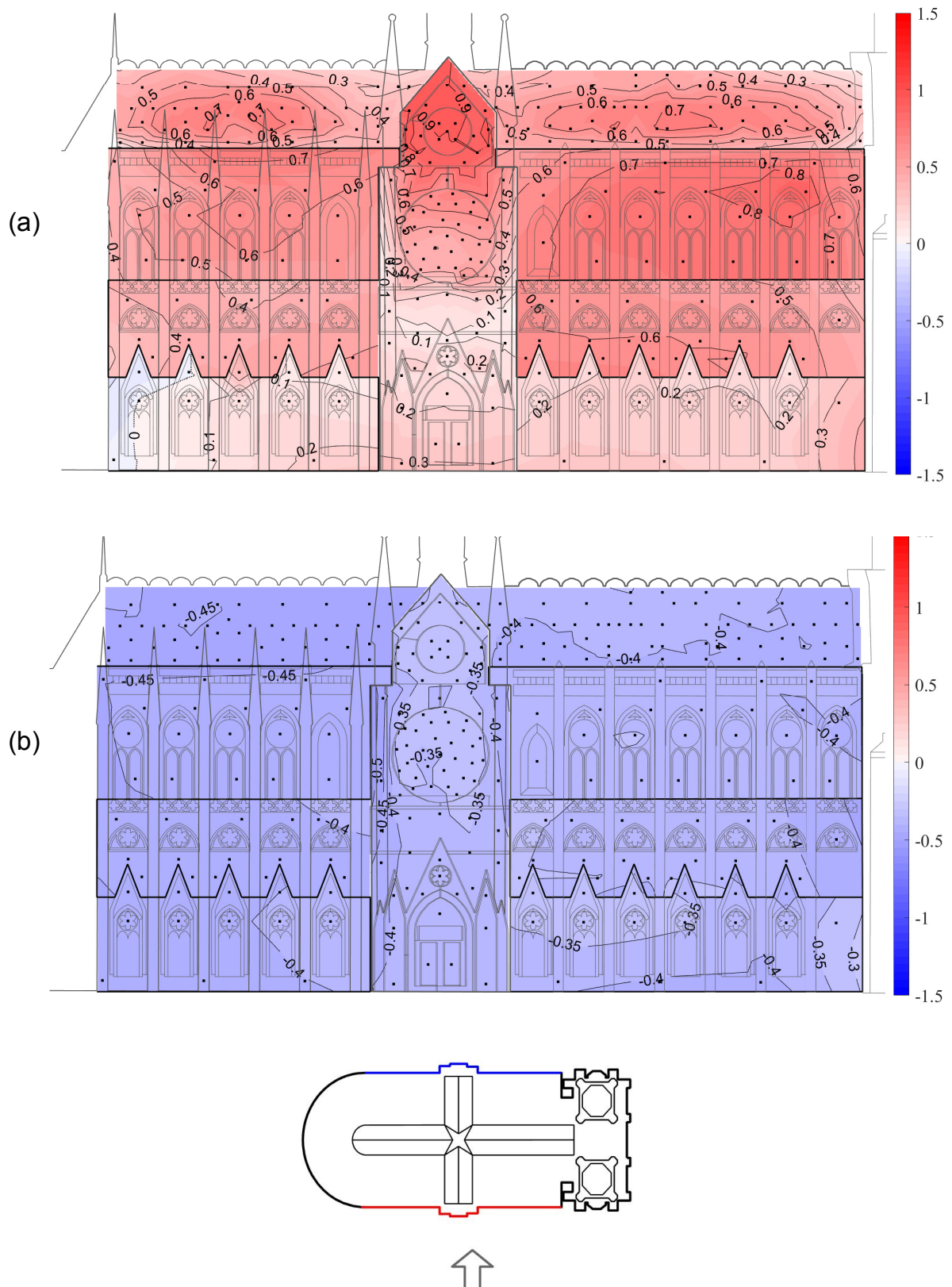


Figure 8: Mean pressure coefficient distribution on the flank of the Cathedral for the configuration with surrounding: windward side (a) and leeward side (b). The wind velocity direction is sketched at the bottom (from North-Northeast, perpendicular to the side walls and denoted as 90° in Fig. 5).

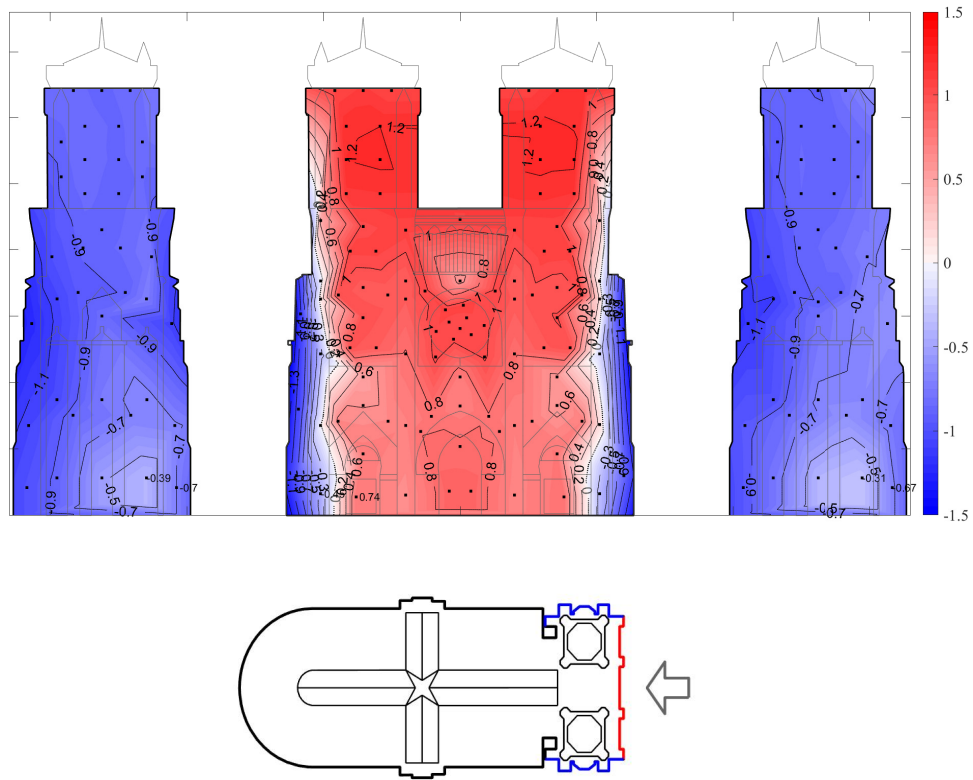


Figure 9: Mean pressure coefficient distribution on the front of the Cathedral and on the external sides of the towers for the configuration with surrounding. The wind velocity direction is sketched at the bottom (from West-Northwest, perpendicular to the main façade and denoted as 0° in Fig. 5).

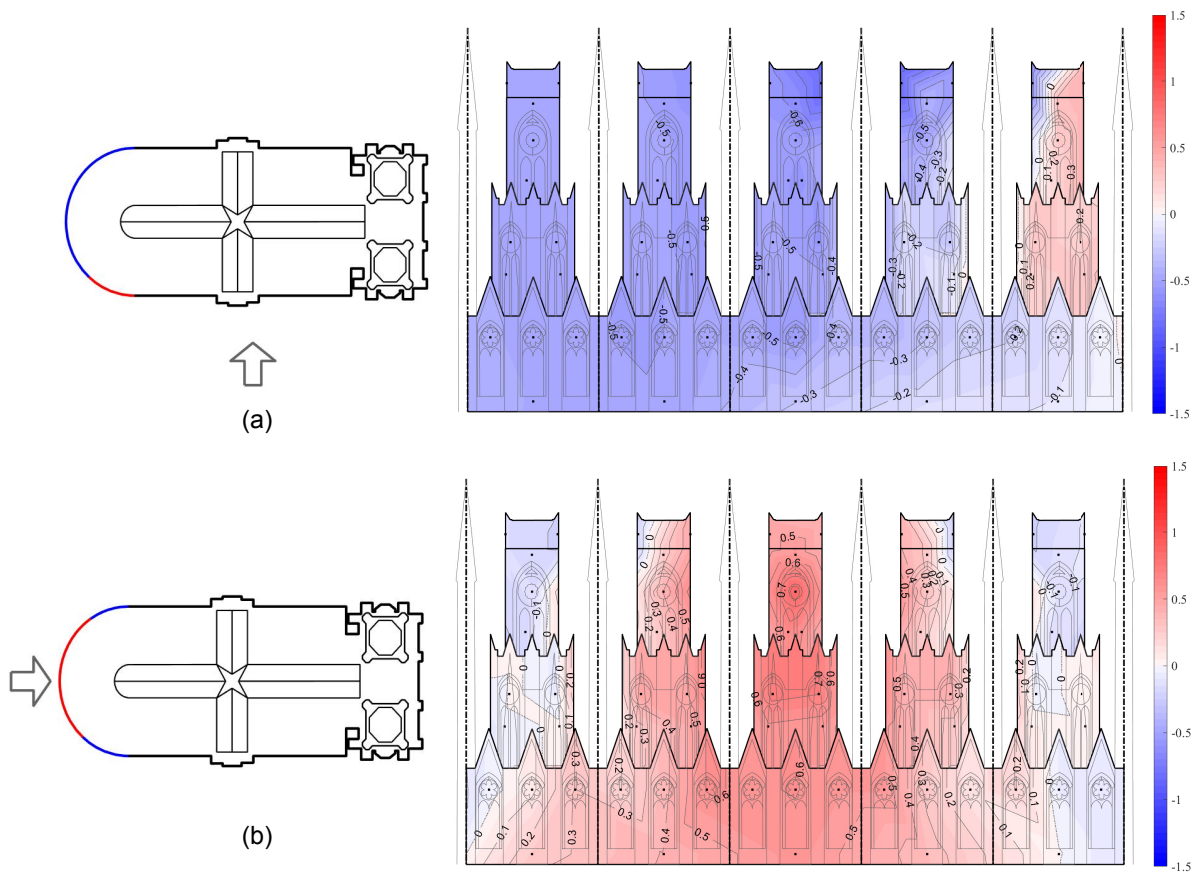


Figure 10: Mean pressure coefficient distribution on the development of the apse of the Cathedral (the curved surface of the Cathedral is unrolled on a plane) for the configuration with surrounding: wind velocity directions of 90° (a) and 180° (b).

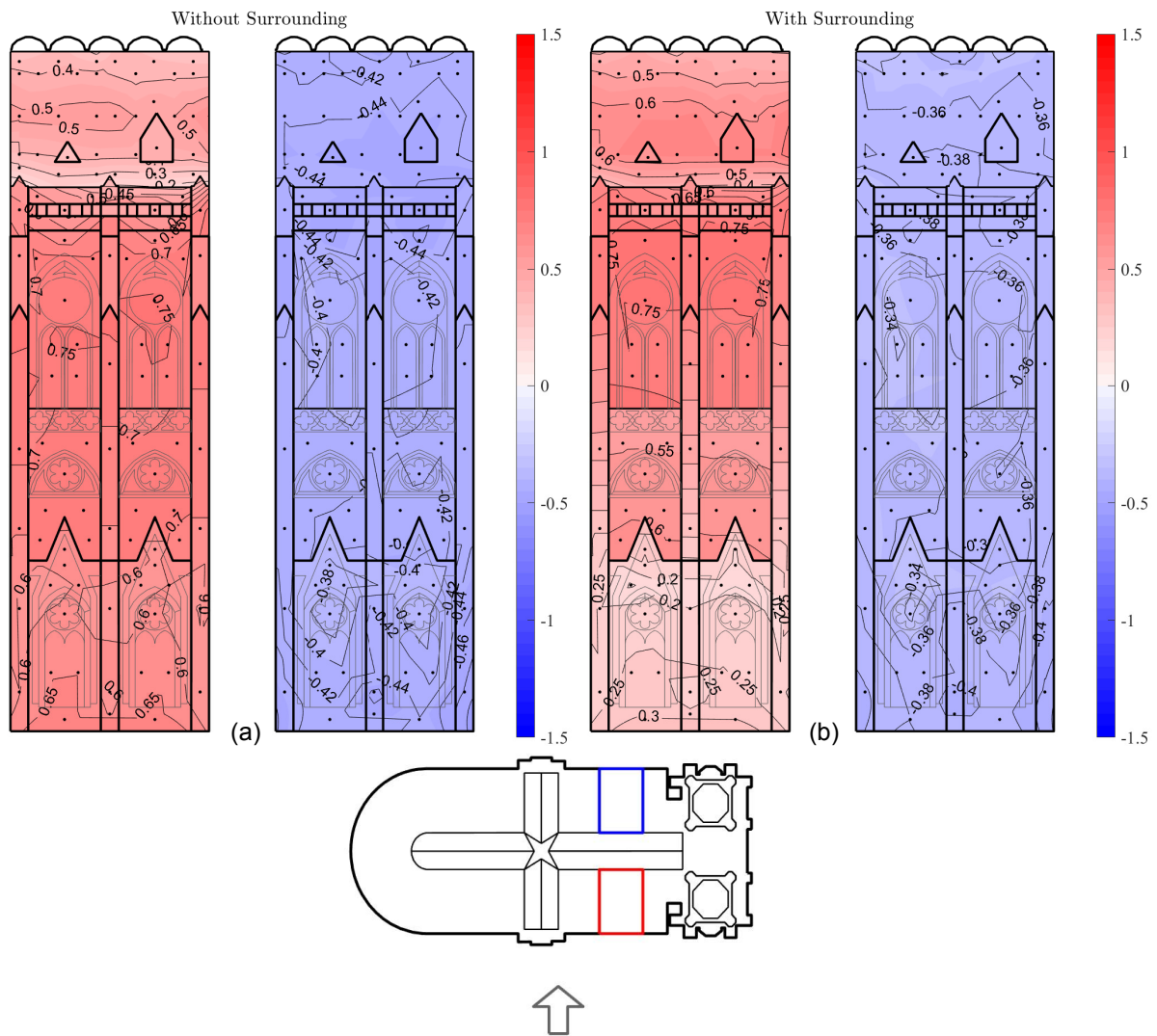


Figure 11: Mean pressure coefficient distribution on a lateral portion of the Cathedral (see Fig. 5) for the configuration without the model of the surrounding (a) and including the buildings around the Cathedral (b). Each frame reports on the left the windward side and on the right the leeward side. The wind velocity direction is sketched at the bottom (perpendicular to the North-Northeast flank, denoted as 90° in Fig. 5).



Figure 12: Flow visualization with a smoke generator in the roof region. The wind direction is perpendicular to the flank of the Cathedral (90°).

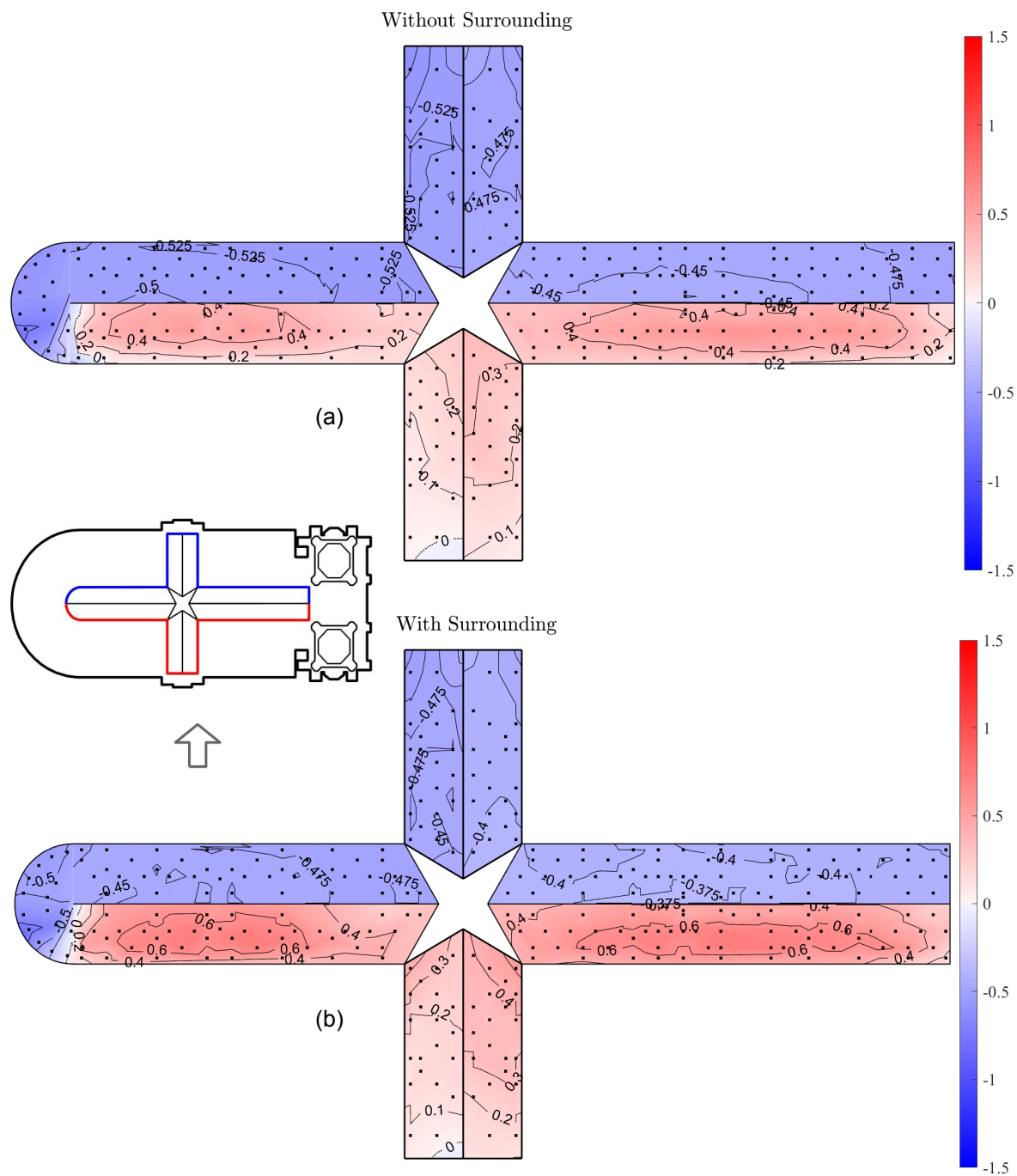


Figure 13: Plan view of the mean pressure coefficients on the roof of the Cathedral: results without surrounding (a) and with surrounding (b). The wind direction, also sketched, is that denoted as 90° in Fig. 5.

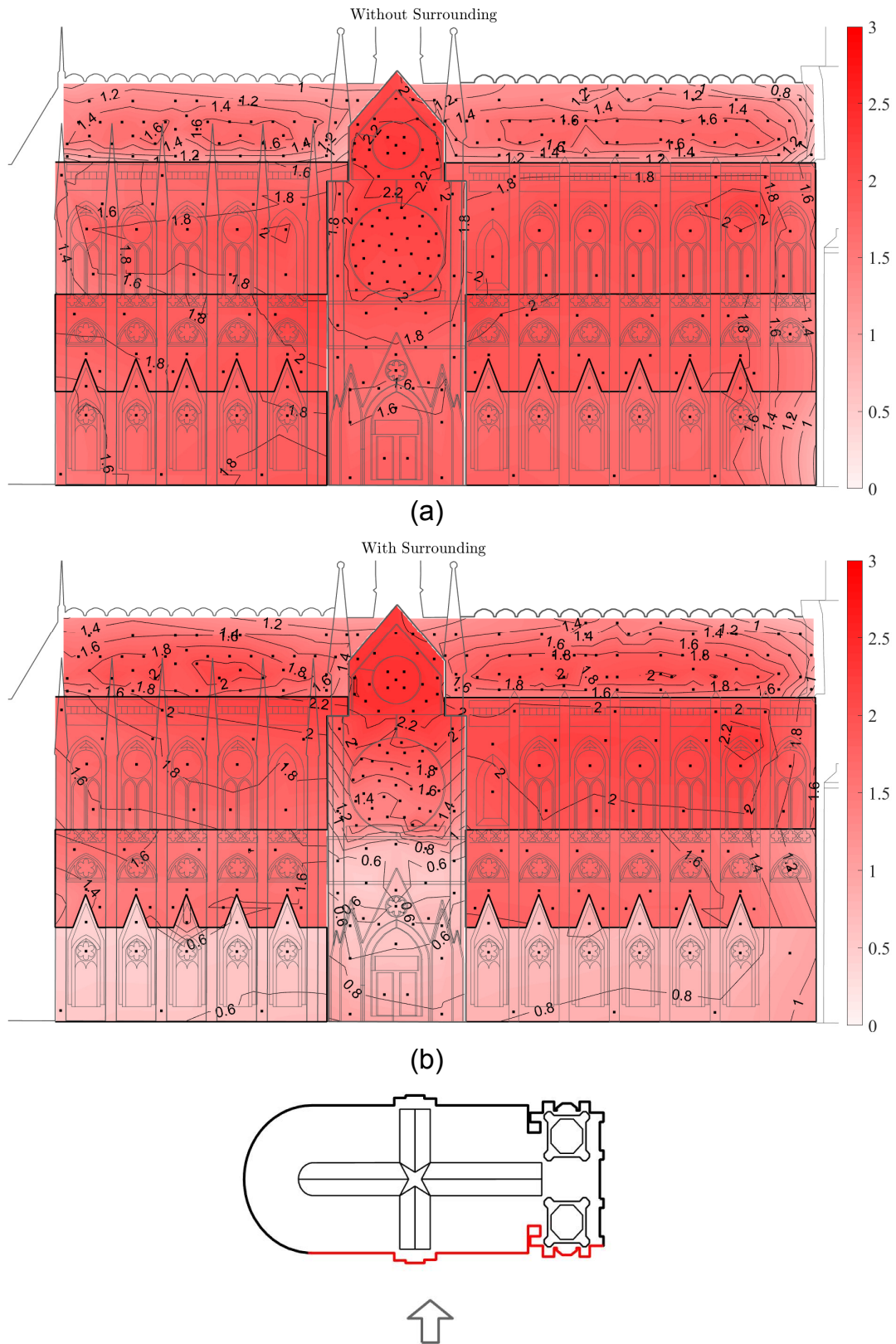


Figure 14: Distribution of the maximum pressure coefficients on the windward flank of the Cathedral for a wind direction perpendicular to it (90° , sketched at the bottom): configuration without surrounding (a) and with surrounding (b).

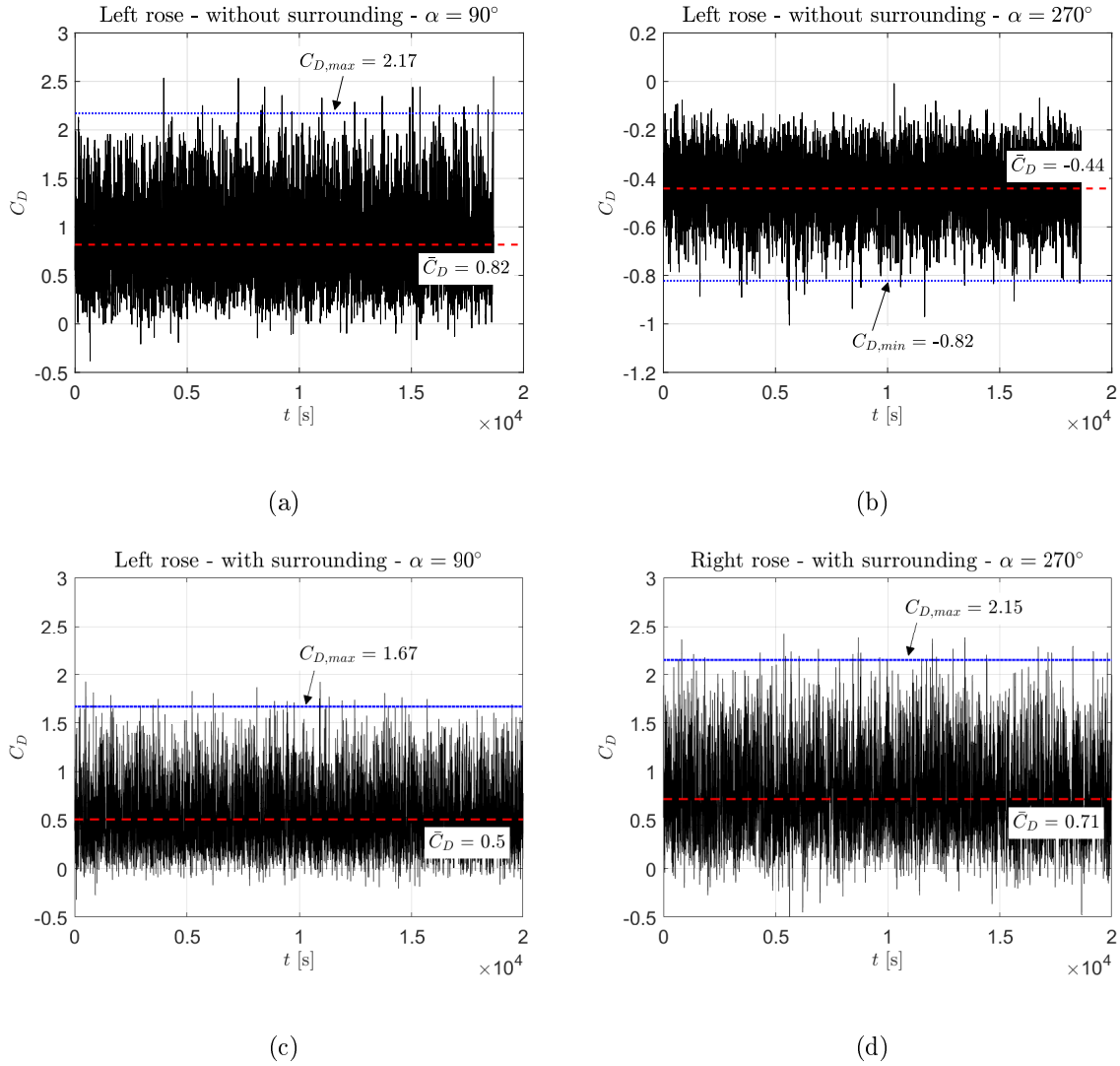


Figure 15: Time history of the integrated force coefficient ($C_D = A^{-1} \int_A C_p dA$, where A denotes the area of the window; time refers to full scale) on the great rose windows of the transept: (a) left rose, wind direction 90° , without surrounding buildings; (b) left rose, wind direction 270° , without surrounding buildings; (c) left rose, wind direction 90° , with surrounding buildings; (d) right rose, wind direction 270° , with surrounding buildings. Both mean and peak values of the load coefficient are reported.

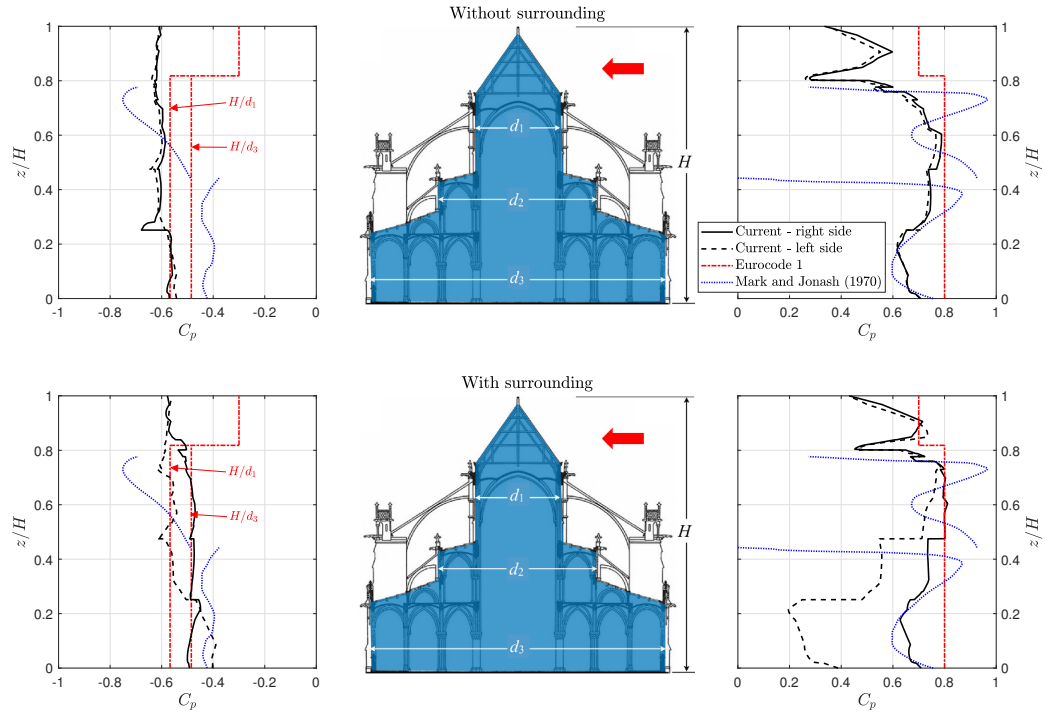


Figure 16: Envelope of mean pressure coefficients along a section of the Cathedral perpendicular to its longitudinal axis for the cases without (top) and with (bottom) surrounding buildings. Comparison with Eurocode 1 (CEN 2004) prescriptions for ordinary buildings and with the data adapted from Mark and Jonash (1970). Windward pressures are reported on the right of the figure, while leeward pressures can be read on the left. “right side” in the caption refers to the nominal wind direction indicated in the schematics (red arrow), whereas “left side” denotes the opposite wind direction.